Direct Metal Laser Sintering Titanium Implants: X-ray Photoelectron Spectroscopy Analysis of Reprocessed Powder

Shaker N, Fernandes A, Fiuza C, França R.

Abstract

Objectives: The aim of the study is to compare the chemical composition of two dental implants manufactured with two kinds of titanium alloys (Ti-6Al-4V) using a 3D printing technique called Direct Metal Laser Sintering (DMLS). The analyses involved two Ti-6Al-4V powders for DMLS: a) the control powder, obtained sealed directly from the manufacturer, not introduced to the production process; b) the experimental powder was recycled powder from the production line.
Materials and Methods: The chemical composition of the control and experimental Titanium alloy powders and the dental implants were determined using X-ray photoelectron spectroscopy (XPS). Three different locations were selected on each of the four samples. Each location selected had 3 chemical composition readings at different depth; 0nm etch, 10nm etch, and 100nm etch. The readings represent the percent composition of the five major components of the titanium alloy powder surface; Oxygen, Carbon, Titanium, Aluminum, Vanadium.
Results: XPS survey analyses show elevated presence of C in the 3D printed implants and no major difference among the major elements Ti, O, V.
Conclusion: 3D printing of Root analogue implants (RAI) is a promising technique that can be used to replace non-restorable teeth as immediate implants.

Keywords Direct Metal Laser sintering (DMLS), Titanium alloy (Ti-6Al-4V)

Introduction

The three most common causes of teeth loss are caries, periodontal disease and vertical root fractures (VRF), respectively. VRF are generally complete, sometimes may be incomplete. [1]
Teeth that have VRF are hopeless and need to be extracted. Immediate implants are the replacement of teeth immediately after extraction with an implant fixture. [2] Advantages of immediately placed implant are, reduced treatment time, preservation of alveolar bone height and width, prevention of resorption post extraction, no additional surgery time and it also has psychological benefits to the patient. On the other hand, there is a higher risk for implant failure, unpredictable hard and soft tissue levels, difficult implant primary stability and bone grafts/membranes often needed. [2]

New advances have been made in the fabrication of Root Analogue Implants (RAI), where prior to the extraction of the non-restorable tooth, the root of a tooth is 3D printed by Direct Metal

Laser Sintering (DMLS) and placed immediately after extraction. The 3D printed implant fitment resembles a key-in a lock type of interaction between the socket and the RAI. [3] This technique eliminates the possibility of needing bone grafts or membrane placement between the immediately placed implant and extraction socket, since the RAI engages the socket completely. [2] The clinician must perform an atraumatic extraction of a non-restorable tooth for a RAI. Any damage to the cortical wall can jeopardize the primary retention of the RAI and reduces the chances of the implant survival. [3]

The process to obtain a RAI for a non-restorable tooth starts by using Cone Beam Computed Tomography (CBCT) pre-extraction. The Digital Imaging and Communication in Medicine (DICOM) files of the CBCT is then converted to a 3D imaging file where the root analogue implant (RAI) is produced by DMLS. [3] 3D printing of the implant by DMLS is building an implant layer by layer via directing a high power laser beam at a bed of Titanium (Ti-6Al-4V) micro particles (25-45µm), which fuses the particles according to a powerful laser beam controlled by a computer aided design (CAD) file. [4] Titanium alloy is used because of its biocompatibility, high strength to weight ration and lower modulus of elasticity, which is compatible with the bone. If there was incompatibility it will cause the bone to resorb, which will cause the implant to loosen.[5] Having the ability to manufacture an implant with gradient of porosity perpendicular to the long axis of the implant helps achieve similar stiffness between the implant and the bone. This helps avoid stress shielding and pressure induced bone loss. A gradient of higher porosity on the outside, which helps with osteointegration and lower porosity in the core, which helps with stiffness, insures similar mechanical properties between bone and implant. [3, 4] In another study a porous core and a dense outer layer implants were 3D printed. Some of the titanium implants produced could have a young modulus of 35 GPa, which is comparable to the young modulus of bone (10 to 30 GPa). The downfall of achieving similar young modulus of titanium to bone is reduced fracture stress of implants [5] Further surface treatments such as sandblasting and acid etching the surface of the implant creates a favorable environment for the implant to osseointegration with the bone. [4, 6]

Osseointegration and biocompatibility of the RAI depends primarily on the chemical surface composition of the titanium alloy. [7] After the DMLS process is complete, the left-over titanium alloy powder is recycled for the subsequent 3D print. This powder, which has been exposed to the manufacturing process, may differ in the surface composition compared to the sealed titanium alloy powder obtained from the manufacturer directly. The biological interaction between the RAI alloy and the bone will vary depending on the percent composition of the alloy components. It has been shown that increasing the content of Al and/or V in the surface composition has increased adhesion of an osteoblast-like cell line through fibronectin-promoted adhesion.[8] Titanium forms a biocompatible surface oxide layer (Mainly TiO_2), which interacts with biological fluids and cells when the implant is placed. This layer is called the passivation layer. The superior osteointegration of titanium is attributed to the passive oxide (TiO_2) layer forming immediately on the surface in air or aqueous solution, which could calcify. In this study, we will be analyzing the effects of the processing on the surface oxide layer of both powders. Comparing the powders (under brand new and reused conditions) and 3D printed RAI samples at 3 different depths will determine the thickness of this passivation

layer. The chemical surface composition of these two different alloys and the thickness of the passivation layer can be used to assess the cytotoxicity of the future manufactured RAI. The null hypothesis is: there is no difference among the chemical composition of the major elements Ti, O, Al, V in the four experimental conditions tested in this study.

Material and methodology

Sampling: Titanium alloy powder (EOS Titanium Ti64, EOS GmbH, Germany) was used in this experiment, under two different conditions; one from the manufacturer directly (brand new, kept under vacuum) and another recycled from previous DMLS process. The DMLS machine used to produce the RAI samples was an EOS M290 (EOS GmbH, Germany) equipped with a Yb fiber laser of 400 W, with a scanning speed up to 7.0 m/s and a focus diameter of 100 μm. All processing was made under an inert gas. After the production, the RAI samples were collected from the tray and stocked in a dry flask to avoid contamination. The powder samples were collected from the sealed flask (control powder) and from the 3D printer tray after at least 20 impressions were processed (used powder).

X-ray photoelectron spectroscopy: Kratos Axis Ultra X-ray Photoelectron Spectroscopy (Wharfside, Manchester, UK) was used to determine the chemical surface composition of the Ti-6Al-4V alloy samples. The parameters used included a base pressure of 2x10-9 torr, an x-ray gun emission set to 15 mA, and an x-ray gun anode HT set to 15 kV, which equates to a power setting of 225 W. The elements detected were observed using both survey and high-resolution spectra. Additional factors included a hybrid lens (magnetic and electrostatic), the use of a charged neutralizer during data acquisition, and aperture set to 700x300μm. A pass energy of 160 eV was used during the survey scan, while a pass energy of 20 eV was used during the high-resolution scan. Data were acquired before etching the samples with argon, as well as after etching at depths of 0 nm, 10 nm, and 100 nm. Casa Software Ltd was used to analyze the XPS results. The analysis was conducted after the XPS binding energy values were calibrated and charge corrected to that of uncharged carbon (CH-CH) at 285.0eV.

Results:

The chemical compositions of the surface of the tested samples are displayed in Table 1. Also figures 1 to 4 show the atomic percentage of the major components (C, O, Ti, Al) according to the probed depth (0 nm, 10 nm, 100 nm).

At the surface (0 nm) the amount of adventitious C was very high in all samples, especially at the implant surfaces (Figure 5). This fact may mask the amount of other major elements: Ti, Al and V. After the etching with Ar, the amount of C was reduced at 10 nm depth (Figure 6) and more significantly at 100 nm (Figure 7). Implant_C present the highest amount of carbon in all three depths.

Table 1. Atomic percentage and standard deviation of the tested samples at surface (0 nm).

	Control Powder		Used Powder		Implant_C		Implant_U	
Elements	**%**	**SD**	**%**	**SD**	**%**	**SD**	**%**	**SD**
O	37.4	1.3	39.4	1.0	21.1	6.4	29.8	6.5
C	44.1	3.3	39.0	1.8	65.9	15.6	47.8	10.4
N	0.8	0.3	0.8	0.3	0.3	0.3	0.7	0.6
Na	0.6	0.4	0.7	0.2	1.1	1.6	0.1	0.1
Ti	9.7	0.8	11.4	1.0	6.2	6.0	8.4	5.0
Si	2.7	0.8	2.7	0.7	1.9	0.7	0.3	0.6
Al	4.6	0.4	5.0	0.3	1.5	1.6	3.8	0.4
Ru	0.0	0.0	1.0	1.8	0.0	0.0	0.0	0.0
Zn	0.0	0.0	0.0	0.0	0.0	0.0	0.6	0.1
Ca	0.0	0.0	0.0	0.0	1.4	0.2	1.3	0.1
V	0.0	0.0	0.0	0.0	0.1	0.1	0.1	0.1
Cu	0.0	0.0	0.0	0.0	0.0	0.0	0.2	0.1
Mg	0.0	0.0	0.0	0.0	0.0	0.0	6.3	1.4
P	0.0	0.0	0.0	0.0	0.0	0.0	0.2	0.4

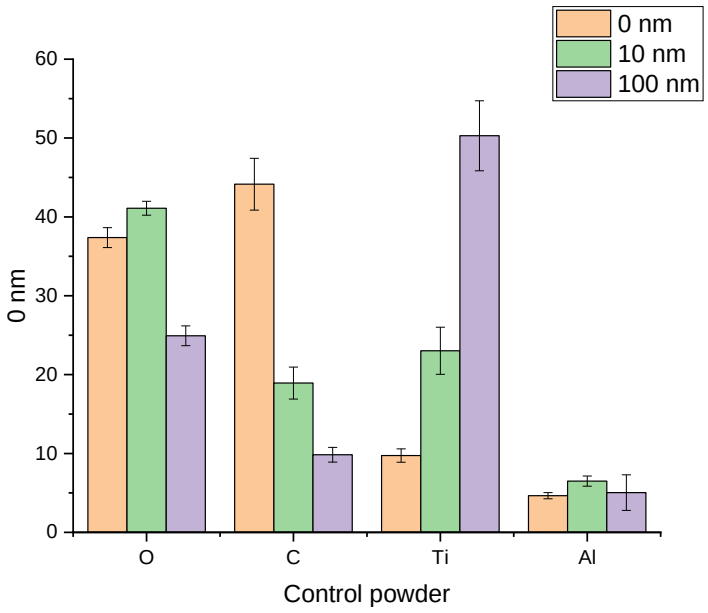

Figure 1. Atomic percentage of the major elements of control powder at three probed depths

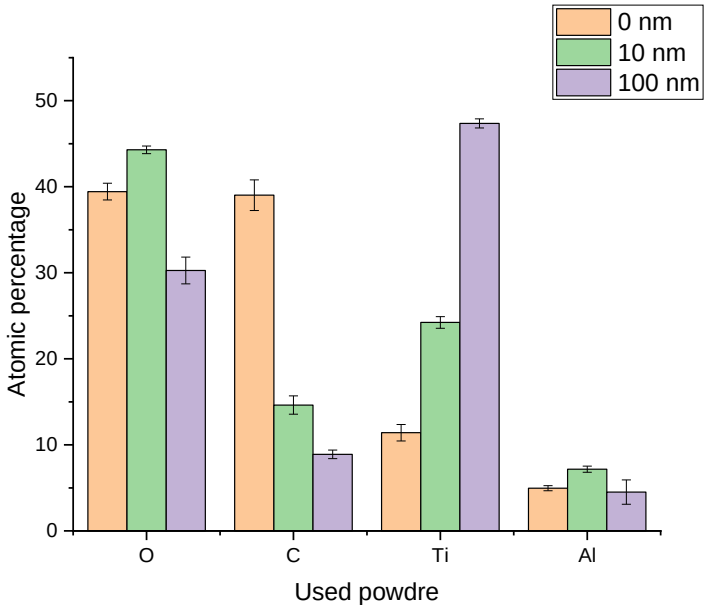

Figure 2. Atomic percentage of the major elements of used powder at three probed depths

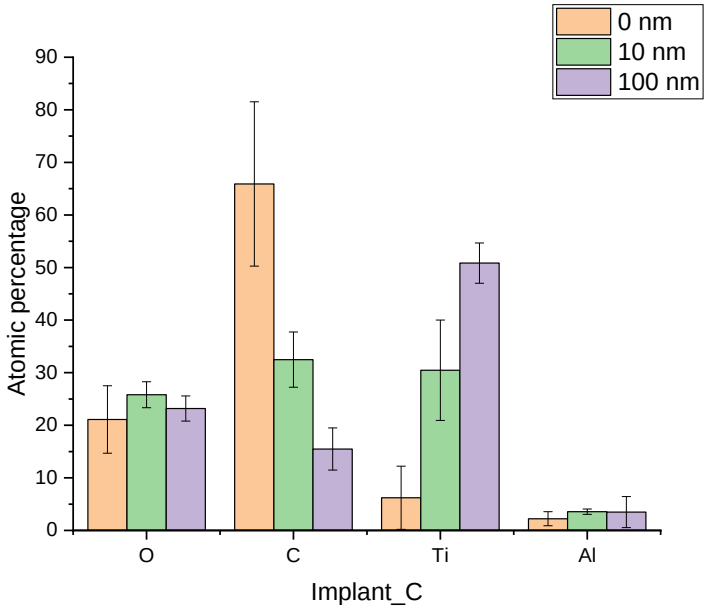

Figure 3. Atomic percentage of the major elements of Implant_C at three probed depths

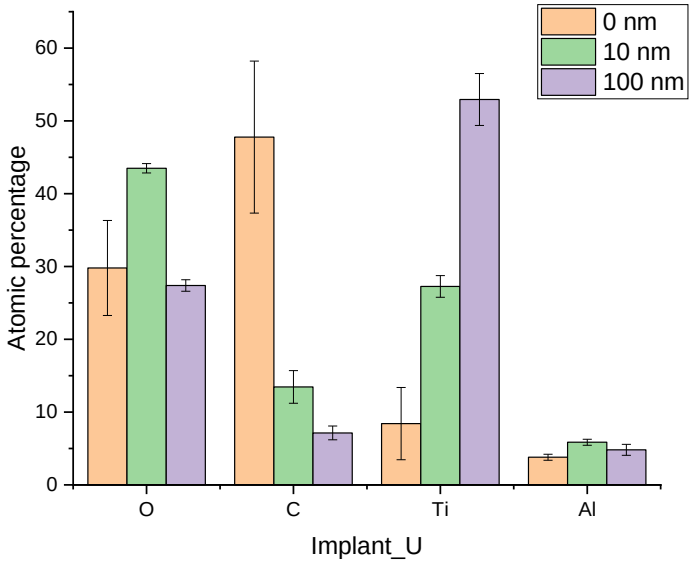

Figure 4. Atomic percentage of the major elements of Implant_U at three probed depths

The amount of O in the three depths were almost the same between the control powder and the used powder, but different from the RAI samples. At implant_C surface, the small amount of O was due to the extra amount of C, as described before. However, at 10 nm depth there was a significant difference between implant_C and implant_U (Figure 6).

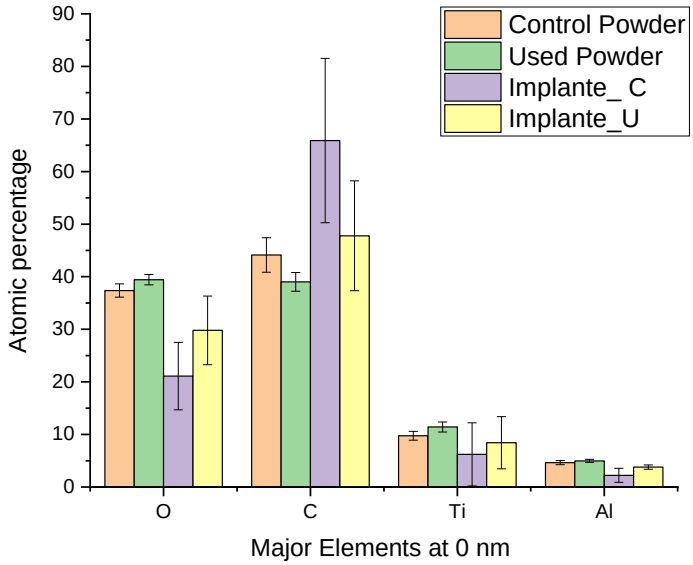

Figure 5. Atomic percentage of the major elements 0 nm depth

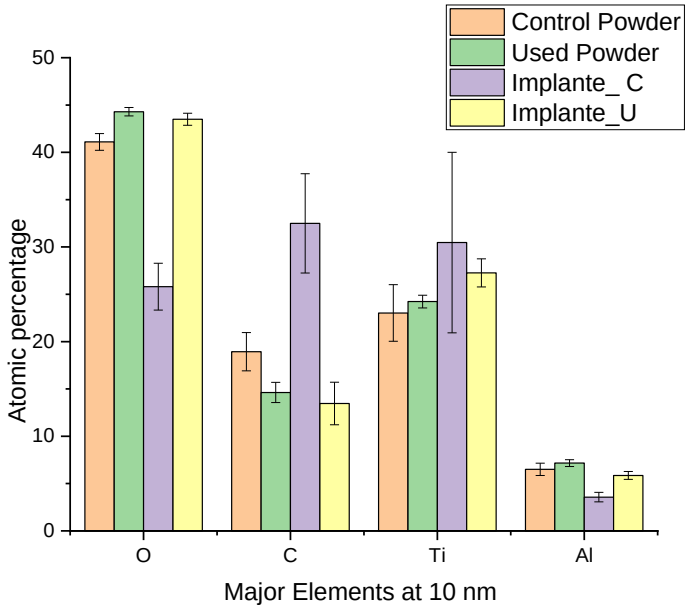

Figure 6. Atomic percentage of the major elements 10 nm depth

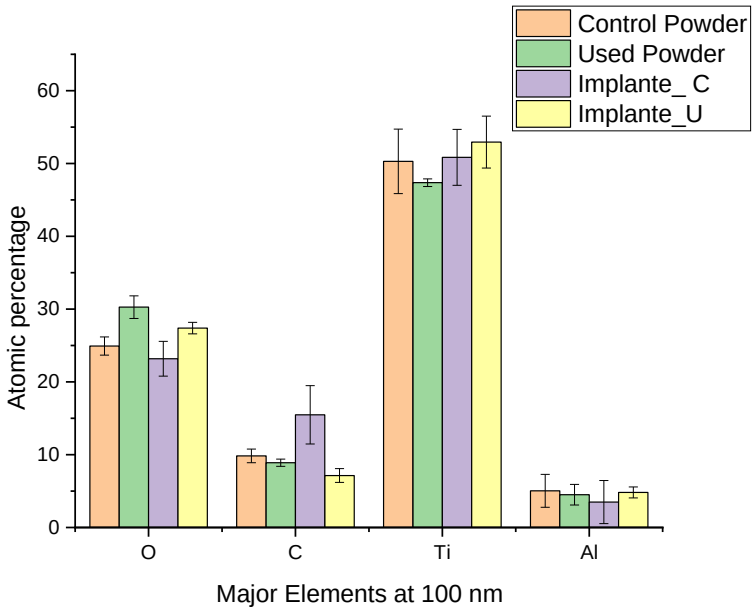

Figure 7. Atomic percentage of the major elements 100 nm depth

The XPS analyses at survey mode did not find major differences in the amount of Ti among all experimental conditions. Small variations for Al was also detected at 10 nm (Fig. 6).

Discussion:

The elevate amount of carbon contamination in the alloy powder and the implants were expected and it comes from the atmosphere. As it is almost impossible to prevent this contamination, the manufacturer recommends using only powder under vacuum conditions to guarantee the purity of the powder. Our results have shown that no major difference was found among the major elements (Ti, O, Al) when a recycle powder was used to produce a 3D dental implant using DMSL technique. So, the null hypothesis was accepted. This finding is excellent news for the future of DMLS. In the contrary case, it would have be forbidden to use recycled power and a necessity to introduce extra steps to treat this powder would generate extra cost.

The clinical relevance of this study: This pioneer study will open the possibility to use DMLS for the production of 3D printed RAI for VRF cases. VRF occur 94% of the time in endodontically treated teeth. [9] Factors that contribute to VRF in endodontically treated teeth are: Forceful lateral condensation during GP placement procedure, excessive dentin removal and wedging forces of endodontic posts. [10, 11] True VRF in non-endodontically treated teeth is rare and was only reported in two studies involving Chinese patients. [10, 12] VRF occurs in roots where the mesio-distal cross-sectional dimension is smaller than the bucco-lingual cross-sectional dimension. That includes maxillary and mandibular pre-molars, mesio-buccal root of mandibular molars, the mandibular anterior teeth and the mesio-buccal roots of the maxillary molars. [13, 14] In the cross-sectional dimension of the root, when dentin is thicker in the bucco-lingual direction than mesio-distal dimension, tensile stresses are variable when stressful forces are applied. This difference in tensile stresses causes more tensile forces on the buccal and lingual dentin walls, which is where the VRF usually occurs. [11] When pressure is applied in a thick-walled vessel, two types of stress occur: tensile stress in a circumferential direction; and compressive stress in a radial direction. The thin part of the wall will be forced to expand more readily than the thick part of the wall in a radial direction. The asymmetrical expansion in a radial direction creates additional circumferential tensile stresses on the inner surface of the thicker areas, which occur in the buccal and lingual dentin wall, resulting from the outward bending of the thinner part of the dentin wall.[11] The crack is usually initiated on the buccal or lingual surface of the inner canal and propagates outwards toward the root surface. Endodontically treated maxillary second pre-molar is the tooth most likely to have a VRF. [15]

3D printed RAI would be an excellent clinical device to restore cases of VRF. However, some preliminary studies must attest the safety of this procedure. The chemical composition of the surface at nanolevel is one of the most important parameters. All reactions that will determine the osteointegration or rejection of the implant will occur at the interface of the alloy and bone. The driving force of these reactions is the interaction between biomolecules (sugars, water and proteins) and the atoms of the outmost layer of the implant. Different chemical compound can modify the speed of the interactions interfering in the results. Also, in order to increase the success rate of immediate implants, patients eligible for such procedures must be selected meticulously. Both soft and hard tissues in the peri-implant area must be

assessed. Alveolar crest ridge width and height should be a minimum of 4 to 5mm and 10mm or more, respectively. These parameters insure stability and adequate distance from vital anatomical structures. [2] Periodontal biotype is a predictor of long term esthetic success of an immediately placed implant. Thick biotypes versus thin biotype have higher chances of success since there is less chance of the tissue receding. [2] Unfortunately, there are no long-term studies about the success or failure of immediate implants compared to delayed placement. [2, 16] Primary retention is an essential requirement for implants. In immediate implants primary retention has been achieved by placing an implant that is 3-5mm longer than the apex of the tooth or an implant that is larger in diameter than the alveolar socket. [2]

Future studies: This study should be confirmed by in-vitro studies that will reveal if the small differences among the experimental condition have an impact on the viability tests. Also, mechanical testing should be performed to determine the physical properties such as elastic modulus, hardness, resistance toughness etc.

Conclusions:

In this experiment the composition of the two different powders were compared and the composition of two RAI made from these two different powders. With the limitations of this experiment, we can conclude that DMLS is a safe method to produce reproducible devices for the dental implantology.

References:

[1] Lubisich EB, Hilton TJ, Ferracane J, Northwest P. Cracked teeth: a review of the literature. J Esthet Restor Dent. 2010;22:158-67.
[2] Koh RU, Rudek I, Wang HL. Immediate implant placement: positives and negatives. Implant Dent. 2010;19:98-108.
[3] Figliuzzi M, Mangano F, Mangano C. A novel root analogue dental implant using CT scan and CAD/CAM: selective laser melting technology. Int J Oral Maxillofac Surg. 2012;41:858-62.
[4] Traini T, Mangano C, Sammons RL, Mangano F, Macchi A, Piattelli A. Direct laser metal sintering as a new approach to fabrication of an isoelastic functionally graded material for manufacture of porous titanium dental implants. Dental materials : official publication of the Academy of Dental Materials. 2008;24:1525-33.
[5] Lin WS, Starr TL, Harris BT, Zandinejad A, Morton D. Additive manufacturing technology (direct metal laser sintering) as a novel approach to fabricate functionally graded titanium implants: preliminary investigation of fabrication parameters. Int J Oral Maxillofac Implants. 2013;28:1490-5.
[6] Zhao G, Raines AL, Wieland M, Schwartz Z, Boyan BD. Requirement for both micron- and submicron scale structure for synergistic responses of osteoblasts to substrate surface energy and topography. Biomaterials. 2007;28:2821-9.

[7] K. Anselme PL, M. Bigerelle. The relative influence of the topography and chemistry of TiAl6V4 surfaces on osteoblastic cell behaviour. Biomaterials. 2000.
[8] MacDonald DE, Rapuano BE, Deo N, Stranick M, Somasundaran P, Boskey AL. Thermal and chemical modification of titanium-aluminum-vanadium implant materials: effects on surface properties, glycoprotein adsorption, and MG63 cell attachment. Biomaterials. 2004;25:3135-46.
[9] Garcia-Guerrero C, Parra-Junco C, Quijano-Guauque S, Molano N, Pineda GA, Marin-Zuluaga DJ. Vertical root fractures in endodontically-treated teeth: A retrospective analysis of possible risk factors. J Investig Clin Dent. 2017.
[10] Chan CP, Lin CP, Tseng SC, Jeng JH. Vertical root fracture in endodontically versus nonendodontically treated teeth: a survey of 315 cases in Chinese patients. Oral Surg Oral Med Oral Pathol Oral Radiol Endod. 1999;87:504-7.
[11] Lertchirakarn V, Palamara JE, Messer HH. Patterns of vertical root fracture: factors affecting stress distribution in the root canal. Journal of endodontics. 2003;29:523-8.
[12] Chan CP, Tseng SC, Lin CP, Huang CC, Tsai TP, Chen CC. Vertical root fracture in nonendodontically treated teeth--a clinical report of 64 cases in Chinese patients. Journal of endodontics. 1998;24:678-81.
[13] Tamse A, Tsesis I, Rosen E. Vertical Root fractures in dentistry.
[14] Haueisen H, Gartner K, Kaiser L, Trohorsch D, Heidemann D. Vertical root fracture: prevalence, etiology, and diagnosis. Quintessence Int. 2013;44:467-74.
[15] Tamse A, Fuss Z, Lustig J, Kaplavi J. An evaluation of endodontically treated vertically fractured teeth. Journal of endodontics. 1999;25:506-8.
[16] Mangano FG, De Franco M, Caprioglio A, Macchi A, Piattelli A, Mangano C. Immediate, non-submerged, root-analogue direct laser metal sintering (DLMS) implants: a 1-year prospective study on 15 patients. Lasers Med Sci. 2014;29:1321-8.